

Effects of environment on stellar metallicity profiles of late-type galaxies in the CALIFA survey

Valeria Coenda^{1,2}, Damián Mast^{2,3}, Hernán Muriel^{1,2}, and Héctor J. Martínez^{1,2}

¹ Instituto de Astronomía Teórica y Experimental (IATE), CONICET - UNC, Laprida 854, X5000BGR, Córdoba, Argentina

² Observatorio Astronómico, Universidad Nacional de Córdoba, Laprida 854, X5000BGR, Córdoba, Argentina.

³ Consejo de Investigaciones Científicas y Técnicas de la República Argentina, Avda. Rivadavia 1917, C1033AAJ, CABA, Argentina.

Received XXXX; accepted XXXX

ABSTRACT

Aims. We explore the effects of environment in the evolution of late-type galaxies by studying the radial profiles of light- and mass-weighted metallicities of galaxies in two discrete environments: field and groups.

Methods. To study the dependence of metallicity on environment. We use a sample of 167 late-type galaxies, with stellar masses $9 \leq \log(M_*/M_\odot) \leq 12$, drawn from the CALIFA survey. Firstly, we obtain light- and mass-weighted stellar metallicity profiles, and stellar mass density profiles of these galaxies, using publicly available data. Then we classify them according to their environment into field and group galaxies. Finally, we make a study of the metallicity of galaxies in these two environments which includes the comparison of the metallicity as a function of the radius, at a characteristic scale, and as a function of the stellar mass surface density. Since metallicity depends on galaxy mass, we take special care throughout the paper in order to compare, in all cases, subsamples of galaxies in groups and in the field that have similar masses.

Results. We find significant differences between group and field late-type galaxies in terms of their metallicity, in the sense that group galaxies are systematically more metallic than their field counterparts. We find that field galaxies have, in general, metallicity profiles that show a negative gradient in their inner regions, and a shallower profile at larger radii. This contrasts with the metallicity profiles of galaxies in groups, which tend to be flat in the inner regions, and to have a negative gradient in the outer parts. Regarding the metallicity at the characteristic radius of the luminosity profiles, we consistently find that it is higher for group galaxies irrespective of galaxy mass. At fixed local stellar surface mass density, group galaxies are again more metallic, also the dependence of metallicity on surface density is less important for group galaxies.

Conclusions. The evidence of a clear difference on the metallicity of group and field galaxies, as a function of mass, spatial scale, and local stellar mass density, are indicative of the different evolutionary paths that galaxies in groups and in the field have followed. We discuss possible implications of the observed differences.

Key words. galaxies: general – galaxies: stellar content – galaxies: evolution – galaxies: groups: general

1. Introduction

The formation and evolution of galaxies is a complicated process that involves the action of different physical mechanisms, acting at different temporal, and spatial scales. As for their origin, these processes can be due to internal or to external, i.e., environmental, factors. There are many internal physical mechanisms that can affect the properties of galaxies, for example, supernovae (SN) outflows (e.g. Stringer et al. 2012, Bower et al. 2012), feedback from massive stars (e.g. Dalla Vecchia & Schaye 2008, Hopkins et al. 2012), active galactic nuclei (AGN) feedback (e.g. Nandra et al. 2007, Hasinger 2008, Silverman et al. 2008, Cimatti et al. 2013), halo heating (Marasco et al. 2012), and morphological quenching (Martig et al. 2009). On the other hand, several environmental mechanisms act upon galaxies at different stages of their life. Galaxies in groups and clusters can lose an important fraction of their cold gas due to the pressure of the intracluster hot gas, a process known as ram pressure stripping (e.g. Gunn & Gott 1972, Abadi et al. 1999, Rasmussen et al. 2006, Jaffé et al. 2012, Hess & Wilcots 2013). The hot gas can also be removed from the galactic halo, cutting off the supply of

gas and consequently stopping star formation, this mechanism is known as starvation (e.g. Larson et al. 1980, Bekki 2009, McCarthy et al. 2008, Bahé et al. 2013, Vijayaraghavan & Ricker 2015). Other mechanisms such as tidal stripping (e.g. Gnedin 2003b, Villalobos et al. 2014), and thermal evaporation (Cowie & Songaila 1977), could be also responsible of affecting galaxy evolution. Galaxy-galaxy high speed interactions (e.g. Moore et al. 1996, Moore et al. 1999, Gnedin 2003a), and mergers, are mechanisms that can redistribute the gaseous, dark matter, and stellar components of a galaxy, with the resulting change in its properties.

Historically, statistical studies of galaxies have been carried out by analysing their integrated properties, such as star formation, metallicity, colour, magnitudes, etc. In recent years, thanks to the new generation of Integral Field Spectroscopy (IFS) surveys such as CALIFA (Sánchez et al. 2012a), SAMI (Bryant et al. 2015), and MANGA (Bundy et al. 2015), it has become possible to obtain a spatially resolved information of the stellar population in galaxies. These instruments have enabled the construction of surveys that include hundreds of galaxies and provide two-dimensional maps for different properties of galaxies,

being the metallicity one of the most studied. The analysis of the spatial distribution of the metallicity inside galaxies, is an important tool to study different physical processes that act at different radii.

Studies of the metallicity distribution in galaxies have been carried out following different approaches and techniques, analysing the gaseous and/or the stellar component. Some of these works have addressed the dependence of metallicity profiles on the environment. However, regardless of the techniques and galaxy samples used, the results continue to be contradictory (Pilyugin & Grebel 2016), and range from finding no difference within 0.02 dex between field and cluster galaxies (Hughes et al. 2013; Kacprzak et al. 2015), to finding that galaxies in clusters are more metallic than those in the field (Shimakawa et al. 2015), or even that star forming (SF) galaxies in clusters are less metallic than those in the field (Valentino et al. 2015). In general, the preferred method to determine the metallicity of SF galaxies, is to measure the oxygen abundance (O/H) in the interstellar medium (ISM) because it is the most abundant heavy element, easy to detect and to obtain measurements for a large sample of galaxies through their emission lines. Without discarding the historical factor that, for the previous reason, make the calibration methods of the abundance relations to be developed and improved with more and better quality data through the years. However, the different calibrators available to determine the gas-phase metallicity (e.g. Pérez-Montero & Díaz 2005; Marino et al. 2013; Pérez-Montero 2017) have a considerable scatter and it may not be easy to determine whether the variations due to the effects of the environment are greater than this scatter. Many studies (e.g. Ellison et al. 2009), prefer gas-phase metallicity because stellar metallicity is insensitive to small variations in metallicity. These authors find variations of 0.02-0.07 dex between different environments. The stellar metallicity accounts for the chemical enrichment throughout the star-forming history of the galaxy. Although HII regions have a memory of the past SFH (Sánchez et al. 2014), gas-phase metallicity is susceptible to outflows and inflows, among others process (Lian et al. 2017; Wu et al. 2017), that can alter the metallicity radial profiles. For this reason, in this paper we have focused on stellar metallicity. Although the expected variations are supposed to be small, we are interested in the evolutionary imprint left by processes acting in different environments. These processes may act on shorter time scales at the ISM, but the imprint of their effect, as far as galactic evolution is concerned, will eventually be on the stellar metallicity. It is important to note that, due to the small variations expected from environmental effects, and given the different processes acting at different radii depending on the morphological type and mass of the galaxies, the best way to study these effects is through a spatially resolved analysis, i.e., a study of integrated properties, as opposed to IFS, may blur any existing evidence of the acting mechanisms.

Several works that use numerical simulations to study the formation and evolution of disks in galaxies favour an inside-out scenario for this component (e.g. Scannapieco et al. 2009; Brook et al. 2012; Tissera et al. 2016). Many observational results using IFS provide support for this. Using the CALIFA survey, Sánchez-Blázquez et al. (2014) find shallow and negative metallicity gradients in disk galaxies. In particular, they find that luminosity-weighted metallicity gradients are steeper than the mass-weighted ones. They also analyse whether the presence of a bar may originate the shallow profiles observed, since bars are supposed to produce stellar migrations (e.g. Wielen 1977, Sellwood & Binney 2002). However, they do not find significant differences between barred and non-barred galaxies,

in disagreement with the predictions of numerical simulations (e.g. Minchev et al. 2012; Di Matteo et al. 2013; Vincenzo & Kobayashi 2020). González Delgado et al. (2016a) also find that spiral galaxies have negative metallicity and age gradients, in agreement with an inside-out formation. Further evidence in favour of the inside-out scenario using CALIFA data is presented in García-Benito et al. (2017). They study the mass assembly time scales of 661 CALIFA galaxies that cover wide ranges in both, mass, and Hubble types. Their results indicate that galaxies form inside-out independently of their stellar mass, stellar mass surface density, and morphology. Lian et al. (2018), using data from the MaNGA survey, also report negative gradients in both, gas, and stellar metallicity, the latter being steeper.

Goddard et al. (2017b) use the MANGA survey to study the internal gradients of the stellar population in galaxies. They obtain negative metallicity gradients for both, early, and late-type galaxies. They find that gradients are steeper for late-types. In addition, Goddard et al. (2017a) analyzed the stellar population properties, age and metallicity, to study the gradients as a function of three characterisations of the environment: local density, tidal strength parameter, and whether a galaxy is central or satellite. In neither case, they find a strong correlation with the environment, and suggest that galaxy mass is the main driver of the stellar population gradients in both, early, and late-types galaxies. Analogously, Zheng et al. (2017) find that the mean age, and metallicity gradients are small however slightly negative. They conclude that their results are consistent with the inside-out formation scenario. These authors also study the environmental dependence of age and metallicity at the effective radii, finding that high-mass galaxies are less affected by the environment.

This paper is the second in a series. In the first paper (Coenda et al. 2019), we explore the effects of environment on the star formation in late-type galaxies, by analysing the radial profiles of the specific star formation rate (sSFR). In that paper, we consider three different environments: field galaxies, galaxies in pairs, and galaxies in groups. Galaxies were selected from the Calar Alto Legacy Integral Field Area (CALIFA).

This article aims to study the effects of the environment over a longer time scale, analysing the stellar metallicity gradients. For this analysis, we use the subsamples of galaxies in groups and in the field, selected by Coenda et al. (2019). This paper is organized as follows: in Sect. 2 we describe in detail our data, namely, the CALIFA data, the environment classification, and the metallicity profiles. In Sect. 3 we present our analysis of the metallicity profiles of late-type galaxies in the field and in groups. Finally, we discuss our results in Sect. 4.

2. The Sample

2.1. CALIFA

One of the the most important integral field surveys of the last decade considering the sample size and the compromise between Field-of-View, spectral coverage, and spatial resolution is the CALIFA Survey. Over five years, more than 900 galaxies were observed. The reduced data, ready for scientific exploitation, were made public in three successive public releases (DR1, Husemann et al. 2013; DR2, García-Benito et al. 2015; DR3, Sánchez et al. 2016). The instrument used was the Potsdam Multi-Aperture Spectrograph (PMAS, Roth et al. 2005) in the PPaK integral field mode (Kelz et al. 2006), mounted on the 3.5m telescope of Calar Alto Observatory. CALIFA observations were performed in two different configurations. On the one hand, using the low resolution V500 grating covering the

wavelength range 3745 – 7500Å, with a spectral resolution of 6.0Å (Full Width Half Maximum, FWHM). The other configuration used the V1200 grating with a medium spectral resolution of 2.3Å (FWHM), in the wavelength range 3650 – 4840Å. The total number of galaxies observed in this second configuration were 484. From the combination of these two configurations, a third data cube called COMBO is obtained with a spectral resolution of 6.0Å, and a wavelength range between 3700 – 7500Å. DR3 made available COMBO data cubes for 446 galaxies.

To construct the CALIFA mother sample, 997 galaxies were selected from the Sloan Digital Sky Survey Data Release 7 photometric galaxy catalogue (SDSS DR7, Abazajian et al. 2009). With an r -band isofotal angular diameter between 45'' – 80'', covering the redshift range $0.005 < z < 0.03$, the CALIFA mother sample covers the color-magnitude diagram and probes a wide range of stellar masses, ionization conditions, and morphological types. The sample morphological classification was performed through visual inspection of the SDSS r -band images by five members of the collaboration. Complete information on the sample characterisation can be found in Walcher et al. (2014). More details on the reduction, observation, and data can be found in Husemann et al. (2013), García-Benito et al. (2015), and Sánchez et al. (2016).

de Amorim et al. (2017) analyzed all DR3 galaxies with COMBO datacubes using the STARLIGHT¹ spectral synthesis code (Cid Fernandes et al. 2005). In combination with the organization code PyCASSO² (Cid Fernandes et al. 2013), they built a catalogue of the stellar populations properties of 445 CALIFA galaxies, providing integrated properties and maps of the stellar mass surface density, mean stellar ages and metallicities, stellar dust attenuation, star formation rates, and kinematics. To perform the analysis of star populations, de Amorim et al. (2017) used two sets of single stellar population (SSP) bases called GMe and CBe, similar to the GM and CB bases presented in Cid Fernandes et al. (2014), but extended in terms of metallicity coverage. As in Coenda et al. (2019), we use in this paper the maps generated with the GMe base which is constructed with a combination of 235 SSP spectra by Vazdekis et al. (2010), for populations over 63 Myr, and the models by González Delgado et al. (2005), for younger ages. The initial mass function used is that of Salpeter (1955), and the metallicity covers the seven bins $(Z/Z_{\odot}) = -2.3, -1.7, -1.3, -0.7, -0.4, 0, +0.22$ (Vazdekis et al. 2010) for SSP over 63Myr, and only the four largest metallicities for younger SSP. The evolutionary tracks are those of Girardi et al. (1993), except for younger ages (1 and 3 Myr) for which Geneva tracks (Schaller et al. 1992) are used instead.

In the present work we study the effects of environment on the stellar metallicity radial profiles of a sample of late-type galaxies with stellar masses in the range $9 \leq \log(M_{\star}/M_{\odot}) \leq 12$, where M_{\star} is the total stellar mass obtained from the integrated spectra as indicated in de Amorim et al. (2017). The sample analyzed in our work consists in a subsample drawn from the DR3 galaxies that have the COMBO data cube and stellar metallicity maps determined.

2.2. Environments

The sample of late-type galaxies used in this paper are a subset of the samples used in Coenda et al. (2019), namely, those that have available metallicity maps, and are either in groups or

in the field. We have excluded for the present paper galaxies in pairs, given the small number of them that have stellar metallicity maps, which made it meaningless to split them into as many different mass bins as we do with group and field galaxies in the next section. Thus, after excluding those galaxies in pairs, we analyse the metallicity profiles of late-type galaxies in groups and in the field.

The three environments explored in Coenda et al. (2019) are defined in terms of a tracer sample of galaxies from the SDSS-DR12 (Alam et al. 2015), with measured redshifts, and restricted to r -band Petrosian magnitudes $r \leq 17.77$. Since the spectroscopic sample of the SDSS is incomplete in redshift for galaxies brighter than $r = 14.5$, in Coenda et al. (2019) the tracer sample is improved with the inclusion of all galaxies in the DR12 photometric database that have no redshift measured by SDSS, but have available redshift in the NED³ database. As CALIFA only observed nearby galaxies ($z < 0.03$), this addition from the NED database improves the level of completeness of the tracer sample, with the consequent improvement of environment characterisation. We describe briefly how groups and field galaxies are defined in Coenda et al. (2019).

2.2.1. Galaxies in groups

Our sample of galaxies in groups includes all CALIFA galaxies that are members of one of the groups of galaxies identified over the tracer sample. Groups of galaxies were identified following Merchán & Zandivarez (2005). For details of group identification we refer the reader to that paper. In brief, the group sample was constructed by means of the algorithm developed by Huchra & Geller (1982) that groups galaxies into systems using a redshift-dependent linking length. This linking length is tuned to retrieve regions with a numerical overdensity of galaxies of 200. A lower limit in membership is imposed, excluding groups with less than four galaxy members. Line-of-sight velocity dispersions are computed using the Gapper estimator in the case of groups with less than 15 members, while for richer groups the bi-weight estimator is used instead (Girardi et al. 1993, 2000). Group virial mass is estimated through the velocity dispersion and the projected virial radius. The resulting sample comprises 17,021 groups with at least four members in the redshift range $0 < z < 0.3$, their virial masses range from $\sim 1 \times 10^{10} M_{\odot}$ to $\sim 1 \times 10^{16} M_{\odot}$ with a median of $\sim 8.5 \times 10^{13} M_{\odot}$. A total of 204 CALIFA galaxies are found to be in these groups, among them, 112 are late-types.

2.2.2. Field galaxies

We consider as field galaxies those CALIFA galaxies that are not included in the group galaxies defined above, and also that are not likely to be part of a pair of galaxies. We explain briefly now, how pairs were defined in Coenda et al. (2019). Firstly, we search among CALIFA galaxies not included in groups, those that are candidate to be in a pair. These are galaxies that have a tracer companion inside a line-of-sight cylinder centered in the CALIFA galaxy and that extends out to a projected radius of 100 kpc, and stretches $\pm 1000 \text{ km s}^{-1}$ in radial velocity (Alpaslan et al. 2015). This results in a candidate list including 127 galaxies, out of which 104 are late-types.

¹ <http://starlight.ufsc.br>

² Python CALIFA Starlight Synthesis organizer, <http://pycasso.ufsc.br>, mirror at <http://pycasso.iaa.es>

³ The NASA/IPAC Extragalactic Database (NED) is operated by the Jet Propulsion Laboratory, California Institute of Technology, under contract with the National Aeronautics and Space Administration, <http://ned.ipac.caltech.edu/>

Secondly, a genuine pair is considered as having the line-of-sight relative velocity of the two galaxies smaller than the escape velocity of a suitable dark matter halo (see details in Coenda et al. 2019) at a distance equal to the projected separation of the galaxies (see also Sales et al. 2007). A total of 77 CALIFA galaxies meet this criterion, out of which 62 are late type. We note that Barrera-Ballesteros et al. (2015), use a less conservative set of parameters than in the present work for defining pairs from the CALIFA sample.

The remaining CALIFA galaxies that were not classified as being part of either, a group or a pair, are considered as field galaxies. These amount to 226 galaxies, including 185 late-types. Some of these galaxies may not be isolated, but in actual in pairs or groups that our procedure has not been able to detect. Thus, the differences we find in the analyses below between field galaxies and group galaxies could actually be more significant. It is, however, unlikely that this possible contamination from galaxies in pairs or groups could change our conclusions.

2.3. Radial profiles of luminosity and metallicity

Following Coenda et al. (2019), for the radial profiles determination, firstly we fit ellipses to the luminosity surface density maps ($\mathcal{L}_{5635\text{\AA}}$) provided by de Amorim et al. (2017). These maps were constructed by directly measuring the average flux of the spectra in the spectral window of $(5635 \pm 45)\text{\AA}$. Using the task ellipse (Jedrzejewski 1987) within IRAF⁴ with 1 spaxel step ($1''$) we obtain the ellipses that we will use later to obtain the metallicity profiles. de Amorim et al. (2017) made available two sets of metallicity maps (measured in solar units), one weighted by luminosity, and the other weighted by mass. We use the ellipses obtained as indicated above as input for a new run of the task ellipse over the metallicity maps. In this way we obtain the metallicity profiles, weighted by mass ($\log(Z_M/Z_\odot)$) and luminosity ($\log(Z_L/Z_\odot)$), that we use to carry out the analyses presented in this paper. We also use the stellar mass surface density, Σ_* , in units of $M_\odot \text{ pc}^{-2}$, calculated from the masses derived with STARLIGHT and provided by de Amorim et al. (2017). This quantity measures the mass currently trapped in stars, as it was corrected for the mass that returned to the interstellar medium during stellar evolution. Our final sample of late-type galaxies with radial metallicity maps comprises 60 galaxies in groups and 107 galaxies in the field. Median values of stellar mass are $\log(M_*/M_\odot) = 10.72$, and 10.70 , for groups, and field galaxies, respectively. As a sanity check of the ellipse step considered, we have redone our analysis with a $2''$ step instead and found that the median of the radial profiles are not altered substantially, thus all conclusions derived here are maintained.

3. Results

We study the effects of external and internal mechanisms on the radial distribution of the metallicity for late-type galaxies. To explore the external effects, we compare late-type galaxies in two discrete environments: field galaxies, and galaxies in groups. To analyse the internal processes, for which mass is the main factor, we split our samples of galaxies into five bins of stellar mass: $\log(M_*/M_\odot) = 9.00 - 10.00$, $10.00 - 10.50$, $10.50 - 10.85$, $10.85 - 11.20$, and $11.20 - 12.00$.

Within each stellar mass bin, the samples of field and group galaxies have, in general, different mass distributions. To avoid mass-related biases in our comparison, we construct subsamples

of field galaxies (the largest of our samples) randomly selected to have a similar mass distribution within each mass bin to that of the group sample. This procedure was performed 50 times for the field galaxies.

Fig. 1 compares radial profiles of light- and mass-weighted stellar metallicity, of galaxies in the field and in groups, split into the five bins of stellar mass mentioned above. The spatial scale is the radius in units of the the r -band half-light effective radius. This effective radius is computed following Graham et al. (2005), involving the SDSS r -band radius that encloses half the Petrosian flux, and the concentration parameter in the same band. We consider the range $0 - 2.5r_e$ to stack the radial profiles and we calculate the median value of r/r_e within each interval of size. The subscript L and M correspond to the metallicity weighing by light and mass, respectively. For galaxies in groups, Fig. 1 shows the median of $\log(Z_{L(M)}/Z_\odot)$ as a function of r/r_e . Vertical error-bars were computed using the bootstrap re-sampling technique. For galaxies in the field, Fig. 1 shows the mean value of the medians of $\log(Z_{L(M)}/Z_\odot)$ as a function of r/r_e , averaged over the 50 random realisations. Error-bars in this case are the dispersion around the mean value. Analogously to González Delgado et al. (2016a) and Coenda et al. (2019), we have considered only mass bins containing more than five galaxies. We quote in all cases the actual number of galaxies contributing to each profile.

In general, we observe in Fig. 1 that $\log(Z_{L(M)}/Z_\odot)$ increases with the stellar mass, and profiles have negative gradients, as has been reported by other authors (e.g. Sánchez-Blázquez et al. 2014, González Delgado et al. 2016a, Goddard et al. 2017b, Zheng et al. 2017, Lian et al. 2018). We find that group galaxies are systematically more metallic than their field counterparts. This is found regardless whether the metallicity is mass-, or luminosity-weighted. For the third stellar mass bin, and for both: the profiles weighted by mass and by luminosity, we observe that galaxies in groups and in the field have similar stellar metallicities. We observe the same trend for the profiles weighted by mass, in the fifth stellar mass bin. With this exceptions, the differences between galaxies in groups and in the field are more noticeable in the luminosity weighted metallicity. Therefore, in what follows, we will centre our analyses in the light-weighted profiles. For mass bins second, fourth and fifth, there is a tendency of the median profiles of the metallicity in groups to have a more flattened metallicity gradient with a negative slope in the outer parts, whereas for field galaxies a more lineal profiles are observed. This results in field and group galaxies having roughly similar metallicities at both extremes: the innermost and the outermost regions. The first mass bin shows a different behavior. Although in this case we also observe that group galaxies have higher metallicity than galaxies in the field, the metallicity profile of the former shows a different shape compared to the other mass bins. In this bin, the metallicity profile of group galaxies presents a convex shape. As a consequence, the differences between the outer and inner radial zones are maximum, and in the middle, the stellar metallicities of both, group, and field galaxies, are similar. Galaxies in this mass bin have the lowest surface brightness. Although we have checked that all galaxies in the bin contribute to the whole range of r/r_e probed, caution should be taken regarding the behaviour in the outermost parts because of a possible low S/N effect.

If we assume that field galaxies have evolved virtually in isolation, or at least, that they have suffered much lesser environmental effects than group galaxies, the differences we observe in the metallicity profiles can be related directly to environmental action.

⁴ <http://iraf.noao.edu/>

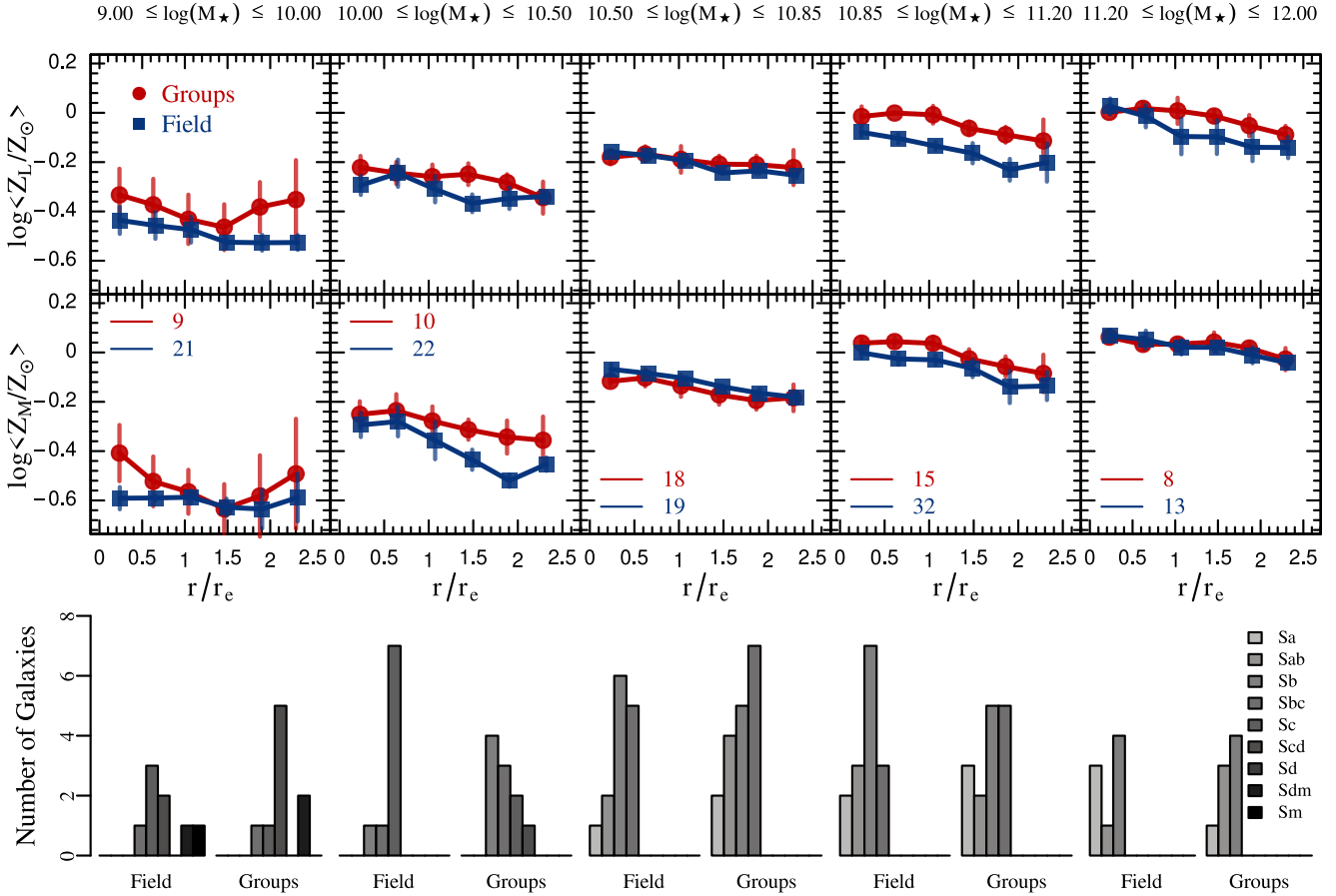


Fig. 1. The stacked profile of the metallicity weighted by light (*top panel*) and mass (*central panel*), for late-type galaxies, scaled to the r -band half-light effective radius, as a function of the mass and the environment. Galaxies in groups are shown as red dots and lines, and field galaxies as blue dots and lines. Red symbols represent the median in each radial size bin for galaxies in groups. Vertical error bars were computed by using the bootstrap re-sampling technique. The blue symbols show the mean value and its dispersion of the field galaxies for 50 randoms runs. *Bottom panel* show the distribution of the Hubble type as a function of the environment and stellar mass. For field galaxies we show the mean distribution for 50 randoms runs performed.

In the bottom panel of Fig. 1 we show the distribution of Hubble types of our sample of late-type galaxies, as a function of stellar mass and environment. For field galaxies we show the average distribution of the 50 randoms runs performed. We observe the morphology distributions are quite similar in both environments for each stellar mass bins. The only probable exception is the second bin of mass, where we observe a tendency of group galaxies to have earlier morphologies than field galaxies. This characteristic of the sample may be partially responsible of the observed differences in metallicity between the two environments. It should be noted that this is the bin of mass that presents the larger difference in metallicity. We also note that each stellar mass bin implies a different set of morphologies. As stellar mass increases, a higher fraction of Sa and Sb galaxies is observed. It is worth noting that the mass-dependent morphological mixing in our samples implies we are not probing an unique galaxy class across the stellar mass range. On the contrary, galaxies in each bin constitute a completely independent sample, and the only common feature bin-to-bin is that galaxies are late-types.

In Coenda et al. (2019) we explore whether AGN feedback, or the presence of a bar, play a role in shaping the sSFR profiles. In contrast to SFR, which involves short timescales, in this work

we are studying the profiles of the stellar metallicities, where different physical mechanisms have acted at different temporal and spatial scales throughout the galaxy lifetime. The size of our sample does not allow for a separate analysis on whether AGNs, or bars, can play a role in the observed stellar metallicity. We observe, however, that the mere presence of an AGN at $z = 0$ does not necessarily imply that it has played a role in shaping the observed galaxy stellar metallicity. An AGN can be a transient phenomenon in a galaxy. With AGN duty cycles spanning timescales in the range $10^6 - 10^8$ yr (Haehnelt & Rees 1993; Davis et al. 2014; Storch-Bergmann & Schnorr-Müller 2019), we expect that the AGN effects on stellar metallicity should be due to past time, not current, AGN activity. Regarding bars, there is no consensus in the literature as to how long do bars last, nor how many bar events an average galaxy has during its lifetime (Sellwood 1999; Athanassoula 2002; Bournaud & Combes 2002; Elmegreen et al. 2004; Combes 2004; Regan & Teuben 2004; Pérez et al. 2008; James & Percival 2016). While several authors have observed a correlation between gas abundance gradients and the presence of bars, in particular, a flattening of the gradient (Vila-Costas & Edmunds 1992; Martin & Roy 1994; Zaritsky et al. 1994), more recent works have found no evidence

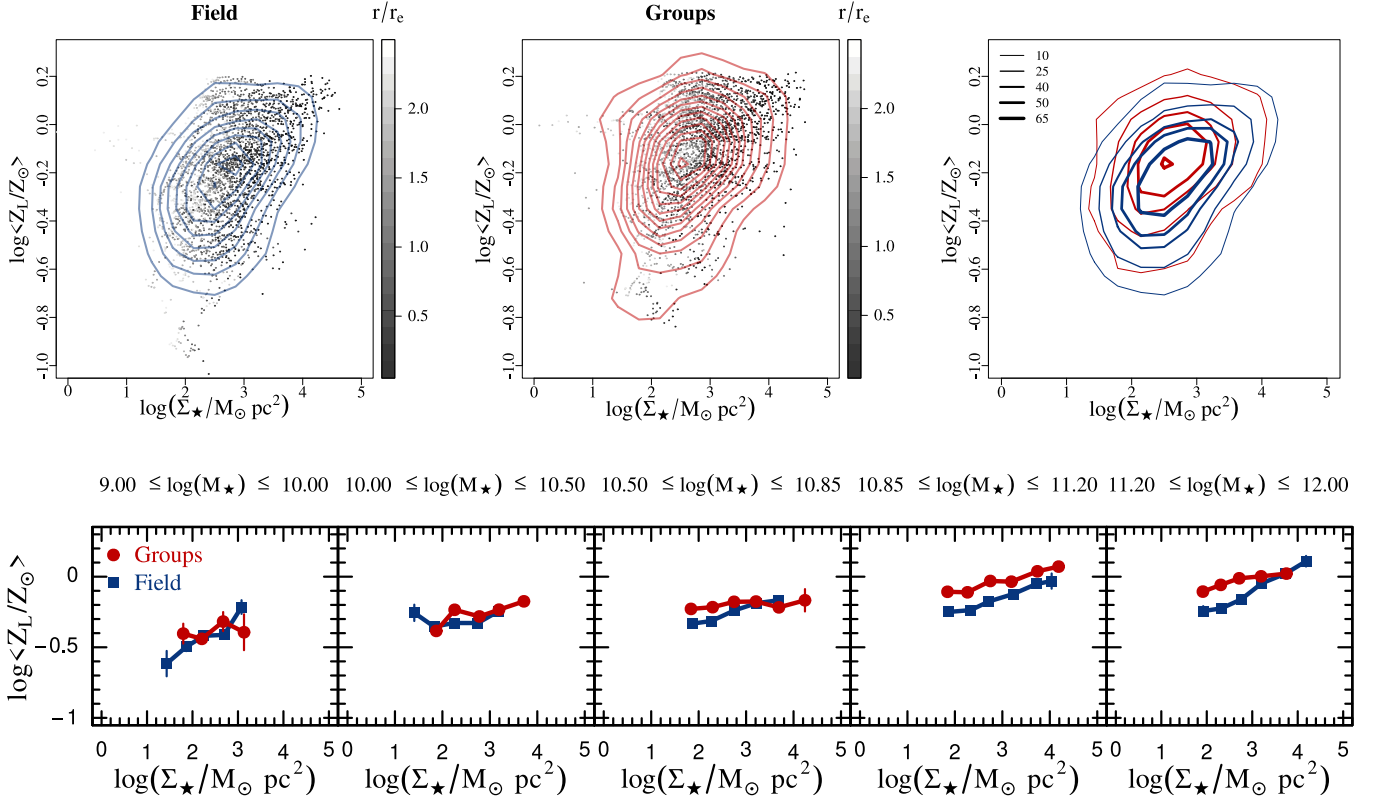


Fig. 2. Top panels: the light-weighted metallicity as a function of the stellar mass surface density Σ_\star . Dots are color-coded in tones of gray according to their distance r/r_e . Left Panel corresponds to galaxies in the field, central panel shows galaxies in groups, and right panel shows the iso-contour levels for galaxies in groups (red lines), and galaxies in the field (blue lines). The bottom panels show the median value of $\log(Z_L/Z_\odot)$ as a function of Σ_\star , for the five stellar mass bins considered. Vertical error bars were computed by using the bootstrap re-sampling technique.

of such a correlation by analyzing both, gas-phase metallicity, and stellar metallicity (Sánchez et al. 2012b, 2014; Sánchez-Blázquez et al. 2014; Cheung et al. 2015; Sánchez-Menguiano et al. 2016).

In the upper panels of Fig. 2 we show the light-weighted metallicity as a function of the stellar mass surface density $\log(\Sigma_\star)$, for galaxies in the field and galaxies in groups. Field galaxies shown in Fig. 2 are a random realization of 107 galaxies from the field sample, selected to have the same overall mass distribution as the group sample. Each galaxy, in any of the two samples, contributes several points to this figure. The number of points vary from galaxy to galaxy, as does the number of radial bins that each profile has. Points are colour-coded in tones of gray according to their radial distance in terms of the effective radius, r/r_e . The solid curves show the number-density iso-contour levels. The stellar mass surface density and metallicity are strongly correlated although we observe significant scatter. To compare galaxies in the field and groups, we show in the upper right panel of Fig. 2, the iso-contour for each environment considered. We clearly observe that galaxies in groups are more metallic for a fixed value of stellar mass surface density.

For a better comparison between group and field galaxies, we split both samples into the 5 mass bins used in Fig. 1 and compute the median value of the $\log(Z_L/Z_\odot)$ as a function of the stellar mass surface density, $\log(\Sigma_\star)$. This is shown in the bottom panels in Fig. 2. Clearly, metallicity depends on both, mass, and stellar mass surface density, i.e., a global, and a local property, respectively. Mass being a major source of scatter in the top panels of this figure. We observe no clear distinction between field and group galaxies in the 2 lowest mass bins. From the third bin

onward, we observe that group galaxies tend to be more metallic at low to intermediate $\log(\Sigma_\star)$ values, although it is not clear that the differences are significant in the third stellar mass bin. Another interesting feature in this figure is that field galaxies tend to have a stronger dependence of metallicity on stellar mass surface density.

A strong correlation between the stellar metallicity and the stellar mass surface density has been reported by Rosales-Ortega et al. (2012), Sánchez et al. (2013), González Delgado et al. (2014). This correlation can be considered as a local process acting in galaxies. Previously, Bell & de Jong (2000), analysed spiral galaxies and found that the stellar mass surface density of galaxies drives its star formation history, and that M_\star is a less important parameter. These previous works argue that stellar metallicities are mainly governed by the stellar mass surface density in disk galaxies, and by the total mass in spheroids. Our results suggest that both, stellar mass surface density, and the integrated stellar mass, impact on the star formation history of late-types galaxies. Moreover, we also find that the environment also plays an important role in modelling the metallicity profiles.

A complementary quantity from our profiles is the metallicity value at r_e . We show in Fig. 3, the median light-weighted stellar metallicity at r_e , as a function of the stellar mass of the galaxy. The metallicity at r_e is correlated with M_\star for late-type galaxies, and this correlation depends on the environment. Low-mass galaxies have lower metallicity than high-mass galaxies. Again, galaxies in groups show a higher value of metallicity than galaxies in the field, for a fixed value of stellar mass. Zheng et al. (2017) find that low-mass galaxies tend to have lower metallicity in low-density environments while high-mass galaxies are less

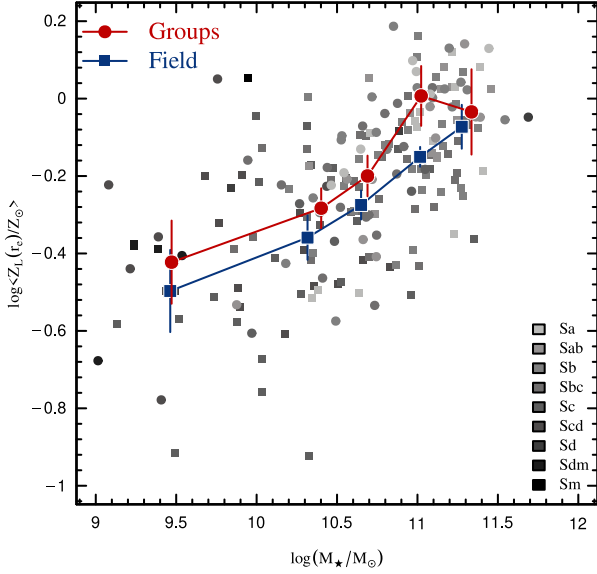


Fig. 3. Light-weighted metallicity at r_e as a function of the stellar mass. Dots are colour-coded in tones of gray according to their Hubble type. The red lines and dots show the median values of $\log(Z_L(r_e)/Z_\odot)$ for galaxies in groups in red, while galaxies in the field are shown in blue.

affected by environment. Our results suggest that the environment affects the metallicities in the whole range of stellar mass, however, future analyses with larger samples are necessary.

4. Discussion and conclusions

In this paper we present a comparative analysis of the stellar metallicity profiles of late-type galaxies in the field and in groups, using publicly available CALIFA data. We focus on three comparative analyses of the metallicity of late-type galaxies: (i) the metallicity profiles in five stellar mass bins, (ii) the relation between metallicity and the stellar mass surface density, (iii) the metallicity at the effective radius. Thus, our analyses compare the metallicity of galaxies as a function of scale (i), at a characteristic scale (iii), and as a function of a local property (ii). As most galaxy properties, including metallicity, depend on galaxy mass, we take special care throughout the paper in order to compare, in all cases, subsamples of galaxies in groups and in the field that have similar mass distributions, within the mass ranges analysed, however broad or thin these ranges might be. In all cases we find significant differences between group and field late-type galaxies. Our results contrast with those of Goddard et al. (2017a), who find that stellar population gradients have no significant correlation with galaxy environment regardless the different characterisations of environment they use. This difference between our results and Goddard et al. (2017a) could be due to our choice of splitting galaxies into two discrete environments.

Regarding the comparison of the radial profiles of metallicity, we find that field galaxies have, in general, metallicity profiles that show a negative gradient in their inner regions, and a shallower profile at larger radii. This contrasts with the metallicity profiles of group galaxies, which tend to be flat in the inner regions, and show a negative gradient in the outer parts. As bulges of late-type galaxies are denser and have stars older than

the disk's, they are expected to be more metallic than the outer parts of the galaxy.

A plausible scenario could be one in which SN ejections, throughout the lifetime of a galaxy, are accreted back into the disk in field galaxies, thus increasing the metallicity of stars formed later in the outer parts of the disk. This should be less efficient in groups due to environmental effects such as ram-pressure stripping or strangulation. Group galaxies have higher metallicity than field galaxies at most scales, and notably at the characteristic radius. Since groups are dense environments, galaxies in groups should, on average, have been formed earlier (i.e. down-sizing), thus having more time to produce metals. On the other hand, mergers are common in groups, and they tend to redistribute metals within galaxies. Furthermore, mergers could add metals to galaxies by the accretion of earlier types satellite galaxies.

Analysing the light-weighted stellar metallicity at r_e , we consistently find that the correlation depends on the environment. Again, galaxies in groups show a higher value of metallicity than galaxies in the field, at a fixed value of stellar mass. These results are consistent with the findings of Zheng et al. (2017), however, in our case the evidence is not only present for low-mass galaxies, but in nearly the entire mass range, being the only exception the highest mass bin, where the median values of metallicities are indistinguishable.

Our analysis of the dependence of metallicity on stellar mass surface density shows that, in general, at fixed local density, group galaxies are more metallic, which backs up the idea that they formed earlier. Another general trend is that the dependence of metallicity on surface density is less important in group galaxies, which may be an indicative of a more effective mix, that can be thought of in terms of more frequent mergers throughout their lifetimes.

As seen in previous works, Σ_\star is a good tracer of the local star population properties where both age and metallicity correlate with Σ_\star (Rosales-Ortega et al. 2012; Sánchez et al. 2013; González Delgado et al. 2014). In particular, in disks Σ_\star would regulate the mean stellar ages and metallicities, while in spheroids, both in spiral bulges and elliptical galaxies, Σ_\star would play a minor role. This is due, as mentioned above, to the fact that in spheroids the chemical enrichment occurred faster and at an earlier stage than in disks, in full correspondence with the inside-out scenario (Pérez et al. 2013; González Delgado et al. 2014, 2015; Sánchez-Blázquez et al. 2014; Sánchez et al. 2014; García-Benito et al. 2017). This would imply that stellar metallicity would be governed by local processes in disks and by global processes in spheroids (González Delgado et al. 2016b). Our Σ_\star analysis shows how, from medium to high densities, which we could associate with spheroids, the effect of the environment is diluted, while the major differences between groups and field occur as Σ_\star decreases. This effect is evidently more noticeable in the medium to high mass bins, bins in which, due to the morphological distribution of the sample, there is a more significant presence of spheroids. This could indicate, therefore, that the environment plays an important role in the chemical evolution of disks and perhaps a minor role in spheroids.

Alongside strong evidences of the universality of the inside-out formation of galaxies, García-Benito et al. (2017) have shown a complex multivariate dependence of the mass assembly on stellar mass, stellar mass surface density, and Hubble type. In Coenda et al. (2019), and in this paper, we have taken special care of these factors in our analyses, and have shown that environment is another factor to reckon with at the time of understanding in detail how galaxies form. In this paper in par-

ticular, we have presented evidence of a clear difference on the metallicity of group and field galaxies, as a function of mass, spatial scale, and local stellar mass density. From an earlier start, a mayor number of mergers experienced during their lifetimes, and the action of other environmental mechanisms, it is clear that late-type galaxies in groups have followed a different evolutionary path, compared to their field counterparts.

Acknowledgements. This paper is based on data obtained by the CALIFA survey (<http://califa.caha.es>) which is based on observations collected at the Centro Astronómico Hispano Alemán (CAHA) at Calar Alto, operated jointly by the Max-Planck-Institut für Astronomie and the Instituto de Astrofísica de Andalucía (CSIC). This research has made use of the NASA/IPAC Extragalactic Database (NED), which is operated by the Jet Propulsion Laboratory, California Institute of Technology, under contract with the National Aeronautics and Space Administration. This paper has been partially supported with grants from Consejo Nacional de Investigaciones Científicas y Técnicas (PIP 11220170100548CO) Argentina, Fondo para la Investigación Científica y Tecnológica (FonCyT, PICT-2017-3301), and Secretaría de Ciencia y Tecnología, Universidad Nacional de Córdoba, Argentina.

References

- Abadi, M. G., Moore, B., & Bower, R. G. 1999, *MNRAS*, 308, 947
- Abazajian, K. N., Adelman-McCarthy, J. K., Agüeros, M. A., et al. 2009, *ApJS*, 182, 543
- Alam, S., Albareti, F. D., Allende Prieto, C., et al. 2015, *ApJS*, 219, 12
- Alpaslan, M., Driver, S., Robotham, A. S. G., et al. 2015, *MNRAS*, 451, 3249
- Athanassoula, E. 2002, in *Astronomical Society of the Pacific Conference Series*, Vol. 275, *Disks of Galaxies: Kinematics, Dynamics and Perturbations*, ed. E. Athanassoula, A. Bosma, & R. Muijica, 141–152
- Bahé, Y. M., McCarthy, I. G., Balogh, M. L., & Font, A. S. 2013, *MNRAS*, 430, 3017
- Barrera-Ballesteros, J. K., García-Lorenzo, B., Falcón-Barroso, J., et al. 2015, *A&A*, 582, A21
- Bekki, K. 2009, *MNRAS*, 399, 2221
- Bell, E. F. & de Jong, R. S. 2000, *MNRAS*, 312, 497
- Bournaud, F. & Combes, F. 2002, *A&A*, 392, 83
- Bower, R. G., Benson, A. J., & Crain, R. A. 2012, *MNRAS*, 422, 2816
- Brook, C. B., Stinson, G. S., Gibson, B. K., et al. 2012, *MNRAS*, 426, 690
- Bryant, J. J., Owers, M. S., Robotham, A. S. G., et al. 2015, *MNRAS*, 447, 2857
- Bundy, K., Bershad, M. A., Law, D. R., et al. 2015, *ApJ*, 798, 7
- Cheung, E., Conroy, C., Athanassoula, E., et al. 2015, *ApJ*, 807, 36
- Cid Fernandes, R., González Delgado, R. M., García Benito, R., et al. 2014, *A&A*, 561, A130
- Cid Fernandes, R., Mateus, A., Sodré, L., Stasińska, G., & Gomes, J. M. 2005, *MNRAS*, 358, 363
- Cid Fernandes, R., Pérez, E., García Benito, R., et al. 2013, *A&A*, 557, A86
- Cimatti, A., Brusa, M., Talia, M., et al. 2013, *ApJL*, 779, L13
- Coenda, V., Mast, D., Martínez, H. J., Muriel, H., & Merchán, M. E. 2019, *A&A*, 621, A98
- Combes, F. 2004, in *IAU Symposium*, Vol. 222, *The Interplay Among Black Holes, Stars and ISM in Galactic Nuclei*, ed. T. Storchi-Bergmann, L. C. Ho, & H. R. Schmitt, 383–388
- Cowie, L. L. & Songaila, A. 1977, *Nature*, 266, 501
- Dalla Vecchia, C. & Schaye, J. 2008, *MNRAS*, 387, 1431
- Davis, B. L., Berrier, J. C., Johns, L., et al. 2014, *ApJ*, 789, 124
- de Amorim, A. L., García-Benito, R., Cid Fernandes, R., et al. 2017, *MNRAS*, 471, 3727
- Di Matteo, P., Haywood, M., Combes, F., Semelin, B., & Snaith, O. N. 2013, *A&A*, 553, A102
- Ellison, S. L., Simard, L., Cowan, N. B., et al. 2009, *MNRAS*, 396, 1257
- Elmegreen, B. G., Elmegreen, D. M., & Hirst, A. C. 2004, *ApJ*, 612, 191
- García-Benito, R., González Delgado, R. M., Pérez, E., et al. 2017, *A&A*, 608, A27
- García-Benito, R., Zibetti, S., Sánchez, S. F., et al. 2015, *A&A*, 576, A135
- Girardi, L., Bressan, A., Bertelli, G., & Chiosi, C. 2000, *A&AS*, 141, 371
- Girardi, M., Biviano, A., Giuricin, G., Madirossian, F., & Mezzetti, M. 1993, *ApJ*, 404, 38
- Gnedin, O. Y. 2003a, *ApJ*, 589, 752
- Gnedin, O. Y. 2003b, *ApJ*, 582, 141
- Goddard, D., Thomas, D., Maraston, C., et al. 2017a, *MNRAS*, 465, 688
- Goddard, D., Thomas, D., Maraston, C., et al. 2017b, *MNRAS*, 466, 4731
- González Delgado, R. M., Cerviño, M., Martins, L. P., Leitherer, C., & Hauschildt, P. H. 2005, *MNRAS*, 357, 945
- González Delgado, R. M., Cid Fernandes, R., García-Benito, R., et al. 2014, *ApJL*, 791, L16
- González Delgado, R. M., Cid Fernandes, R., Pérez, E., et al. 2016a, *A&A*, 590, A44
- González Delgado, R. M., Cid Fernandes, R., Pérez, E., et al. 2016b, *A&A*, 590, A44
- González Delgado, R. M., García-Benito, R., Pérez, E., et al. 2015, *A&A*, 581, A103
- Graham, A. W., Driver, S. P., Petrosian, V., et al. 2005, *AJ*, 130, 1535
- Gunn, J. E. & Gott, J. R. I. 1972, *ApJ*, 176, 1
- Haehnelt, M. G. & Rees, M. J. 1993, *MNRAS*, 263, 168
- Hasinger, G. 2008, *A&A*, 490, 905
- Hess, K. M. & Wilcots, E. M. 2013, *AJ*, 146, 124
- Hopkins, P. F., Quataert, E., & Murray, N. 2012, *MNRAS*, 421, 3522
- Huchra, J. P. & Geller, M. J. 1982, *ApJ*, 257, 423
- Hughes, T. M., Cortese, L., Boselli, A., Gavazzi, G., & Davies, J. I. 2013, *A&A*, 550, A115
- Husemann, B., Jahnke, K., Sánchez, S. F., et al. 2013, *A&A*, 549, A87
- Jaffé, Y. L., Poggianti, B. M., Verheijen, M. A. W., Deshev, B. Z., & van Gorkom, J. H. 2012, *ApJL*, 756, L28
- James, P. A. & Percival, S. M. 2016, *MNRAS*, 457, 917
- Jedrzejewski, R. I. 1987, *MNRAS*, 226, 747
- Kacprzak, G. G., Yuan, T., Nanayakkara, T., et al. 2015, *ApJL*, 802, L26
- Kelz, A., Verheijen, M. A. W., Roth, M. M., et al. 2006, *PASP*, 118, 129
- Larson, R. B., Tinsley, B. M., & Caldwell, C. N. 1980, *ApJ*, 237, 692
- Lian, J., Thomas, D., Maraston, C., et al. 2018, *MNRAS*, 476, 3883
- Lian, J., Yan, R., Blanton, M., & Kong, X. 2017, *MNRAS*, 472, 4679
- Marasco, A., Fraternali, F., & Binney, J. J. 2012, *MNRAS*, 419, 1107
- Marino, R. A., Rosales-Ortega, F. F., Sánchez, S. F., et al. 2013, *A&A*, 559, A114
- Martig, M., Bournaud, F., Teyssier, R., & Dekel, A. 2009, *ApJ*, 707, 250
- Martin, P. & Roy, J.-R. 1994, *ApJ*, 424, 599
- McCarthy, I. G., Frenk, C. S., Font, A. S., et al. 2008, *MNRAS*, 383, 593
- Merchán, M. E. & Zandivarez, A. 2005, *ApJ*, 630, 759
- Minchev, I., Famaey, B., Quillen, A. C., et al. 2012, *A&A*, 548, A127
- Moore, B., Katz, N., Lake, G., Dressler, A., & Oemler, A. 1996, *Nature*, 379, 613
- Moore, B., Lake, G., Quinn, T., & Stadel, J. 1999, *MNRAS*, 304, 465
- Nandra, K., Georgakakis, A., Willmer, C. N. A., et al. 2007, *ApJL*, 660, L11
- Pérez, E., Cid Fernandes, R., González Delgado, R. M., et al. 2013, *ApJL*, 764, L1
- Pérez, I., Sánchez-Blázquez, P., & Zurita, A. 2008, in *Astronomical Society of the Pacific Conference Series*, Vol. 396, *Formation and Evolution of Galaxy Disks*, ed. J. G. Funes & E. M. Corsini, 375
- Pérez-Montero, E. 2017, *PASP*, 129, 043001
- Pérez-Montero, E. & Díaz, A. I. 2005, *MNRAS*, 361, 1063
- Pilyugin, L. S. & Grebel, E. K. 2016, *MNRAS*, 457, 3678
- Rasmussen, J., Ponman, T. J., & Mulchaey, J. S. 2006, *MNRAS*, 370, 453
- Regan, M. W. & Teuben, P. J. 2004, *ApJ*, 600, 595
- Rosales-Ortega, F. F., Sánchez, S. F., Iglesias-Páramo, J., et al. 2012, *ApJL*, 756, L31
- Roth, M. M., Kelz, A., Fechner, T., et al. 2005, *PASP*, 117, 620
- Sales, L. V., Navarro, J. F., Abadi, M. G., & Steinmetz, M. 2007, *MNRAS*, 379, 1475
- Salpeter, E. E. 1955, *ApJ*, 121, 161
- Sánchez, S. F., García-Benito, R., Zibetti, S., et al. 2016, *A&A*, 594, A36
- Sánchez, S. F., Kennicutt, R. C., Gil de Paz, A., et al. 2012a, *A&A*, 538, A8
- Sánchez, S. F., Rosales-Ortega, F. F., Iglesias-Páramo, J., et al. 2014, *A&A*, 563, A49
- Sánchez, S. F., Rosales-Ortega, F. F., Jungwiert, B., et al. 2013, *A&A*, 554, A58
- Sánchez, S. F., Rosales-Ortega, F. F., Marino, R. A., et al. 2012b, *A&A*, 546, A2
- Sánchez-Blázquez, P., Rosales-Ortega, F. F., Méndez-Abreu, J., et al. 2014, *A&A*, 570, A6
- Sánchez-Menguiano, L., Sánchez, S. F., Pérez, I., et al. 2016, *A&A*, 587, A70
- Scannapieco, C., White, S. D. M., Springel, V., & Tissera, P. B. 2009, *MNRAS*, 396, 696
- Schaller, G., Schaerer, D., Meynet, G., & Maeder, A. 1992, *A&AS*, 96, 269
- Sellwood, J. A. 1999, in *Astronomical Society of the Pacific Conference Series*, Vol. 182, *Galaxy Dynamics - A Rutgers Symposium*, ed. D. R. Merritt, M. Valluri, & J. A. Sellwood, 96
- Sellwood, J. A. & Binney, J. J. 2002, *MNRAS*, 336, 785
- Shimakawa, R., Kodama, T., Tadaki, K.-i., et al. 2015, *MNRAS*, 448, 666
- Silverman, J. D., Mainieri, V., Lehmer, B. D., et al. 2008, *ApJ*, 675, 1025
- Storchi-Bergmann, T. & Schnorr-Müller, A. 2019, *Nature Astronomy*, 3, 48
- Stringer, M. J., Bower, R. G., Cole, S., Frenk, C. S., & Theuns, T. 2012, *MNRAS*, 423, 1596
- Tissera, P. B., Machado, R. E. G., Sanchez-Blazquez, P., et al. 2016, *A&A*, 592, A93
- Valentino, F., Daddi, E., Strazzullo, V., et al. 2015, *ApJ*, 801, 132
- Vazdekis, A., Sánchez-Blázquez, P., Falcón-Barroso, J., et al. 2010, *MNRAS*, 404, 1639
- Vijayaraghavan, R. & Ricker, P. M. 2015, *MNRAS*, 449, 2312
- Vila-Costas, M. B. & Edmunds, M. G. 1992, *MNRAS*, 259, 121
- Villalobos, A., De Lucia, G., & Murante, G. 2014, *MNRAS*, 444, 313
- Vincenzo, F. & Kobayashi, C. 2020, arXiv e-prints, arXiv:2004.08050
- Walcher, C. J., Wisotzki, L., Bekeraite, S., et al. 2014, *A&A*, 569, A1
- Wielen, R. 1977, *A&A*, 60, 263
- Wu, P.-F., Zahid, H. J., Hwang, H. S., & Geller, M. J. 2017, *MNRAS*, 468, 1881
- Zaritsky, D., Kennicutt, Robert C., J., & Huchra, J. P. 1994, *ApJ*, 420, 87
- Zheng, Z., Wang, H., Ge, J., et al. 2017, *MNRAS*, 465, 4572